Computer Physics Communications 209 (2016) 42–47

Contents lists available at ScienceDirect

Computer Physics Communications

journal homepage: www.elsevier.com/locate/cpc

The digital computer as a metaphor for the perfect laboratory experiment: Loophole-free Bell experiments

Hans De Raedt [a], Kristel Michielsen [b,*], Karl Hess [c]

[a] Zernike Institute for Advanced Materials, University of Groningen, Nijenborgh 4, NL-9747 AG Groningen, The Netherlands
[b] Institute for Advanced Simulation, Jülich Supercomputing Centre, Forschungzentrum Jülich, D-52425 Jülich, Germany
[c] Center for Advanced Study, University of Illinois, Urbana, IL, United States

ARTICLE INFO

Article history:
Received 11 June 2016
Received in revised form
9 August 2016
Accepted 11 August 2016
Available online 18 August 2016

Keywords:
Discrete event simulation
Foundations of quantum mechanics
Bell inequalities

ABSTRACT

Using Einstein–Podolsky–Rosen–Bohm experiments as an example, we demonstrate that the combination of a digital computer and algorithms, as a metaphor for a perfect laboratory experiment, provides solutions to problems of the foundations of physics. Employing discrete-event simulation, we present a counterexample to John Bell's remarkable "proof" that any theory of physics, which is both Einstein-local and "realistic" (counterfactually definite), results in a strong upper bound to the correlations that are being measured in Einstein–Podolsky–Rosen–Bohm experiments. Our counterexample, which is free of the so-called detection-, coincidence-, memory-, and contextuality loophole, violates this upper bound and fully agrees with the predictions of quantum theory for Einstein–Podolsky–Rosen–Bohm experiments.

1. Introduction

Digital computers are physical devices, the state of which changes according to well-defined rules. Executing an algorithm on a digital computer is an experiment in which there are no unknown factors that might affect the outcome. Therefore the digital computer + algorithm can be viewed as a metaphor for a perfect laboratory experiment.

Moreover there always exists a one-to-one mapping from the state of the computer to objects that are directly accessible to our senses. Therefore computer simulation offers unique possibilities to confront man-made concepts and theories with actual facts, real perfect experiments, not just abstract symbols, thereby facilitating the ordering and deeper understanding of human experience.

In view of this potential it is surprising that a general feeling exists that computer simulation cannot contribute much to the foundations of quantum physics. This is somewhat remarkable because in other important subfields of theoretical physics, such as statistical physics, computer simulation has proven essential in advancing the field [1].

In the present paper, we use the "computer"-"laboratory experiment" metaphor to perform discrete-event simulations of a loophole-free idealization of the Einstein–Podolsky–Rosen–Bohm (EPRB) experiment of Weihs et al. [2]. The simulation model which complies with the notions of Einstein locality and counterfactual definiteness generates data that is in full agreement with quantum theory, demonstrating that (i) counterfactual definiteness or a Bell-type inequality does not separate classical from quantum physics and (ii) a violation of a Bell-type inequality points to a deficiency of the applicability and connection of the mathematical axiomatic system (that is used for Bell's derivation) to the data (see also [3]).

Counterfactual "measurements" yield values that have been derived by means other than direct observation or actual measurement, such as by calculation on the basis of a well-substantiated theory. If one knows an equation that permits deriving reliably expected values from a list of inputs to the physical system under investigation, then one has "counterfactual definiteness" (CFD) in the knowledge of that system. For an extensive discussion of counterfactuals see Ref. [4].

The derivation of the Theorem of Bell and Bell's inequality necessitate the postulate of CFD [5]. In the present paper we adopt the definition of CFD as given in an earlier paper [5]:

> A counterfactually definite theory is described by a function (or functions) that map(s) tests onto numbers. The variables of the function(s) argument must be chosen in a one to one correspondence to physical entities that describe the test(s) and must be independent variables in the sense that they can be arbitrarily chosen from their respective domains.

* Corresponding author.
E-mail address: k.michielsen@fz-juelich.de (K. Michielsen).

http://dx.doi.org/10.1016/j.cpc.2016.08.010

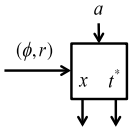

Fig. 1. Block diagram of an observation station. The input–output relations $x = x(a, \phi)$ and $t^* = t^*(a, \phi, r)$ are defined by Eqs. (1) and (2).

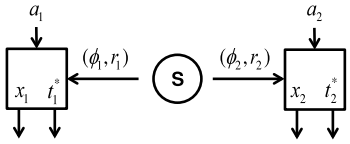

Fig. 2. Schematic layout of the computational equivalent of a laboratory EPRB experiment [2,9]. The input–output relation for $i = 1, 2$ is given by $x_i = x(a_i, \phi_i)$ and $t_i^* = t^*(a_i, \phi_i, r_i)$ where $x = x(a, \phi)$ and $t^* = t^*(a, \phi, r)$ are defined by Eqs. (1) and (2). Alternatively, the input–output relation may be written as $(x_1, t_1^*, x_2, t_2^*) = F(\phi_1, \phi_2, r_1, r_2, a_1, a_2)$ showing that for fixed (a_1, a_2) the simulation model satisfies the definition of a CFD theory [5].

In brief, CFD means that the output state of a system can, in principle, be calculated using an explicit formula, e.g. $y = f(x)$ where $f(.)$ is a known (vector-valued) function of its argument x. If x denotes a vector of values then, according to the above definition, the elements of this vector must be independent variables for the mathematical model to be CFD-compliant.

Although it is clear that CFD cannot be tested in a conventional laboratory experiment [6], a digital computer is nothing but a physical device that performs a kind of experiment (e.g. flipping bits), albeit one that is under perfect control (we assume that the computer is operating flawless). Therefore a digital computer may be used as a metaphor for carrying out ideal, perfect experiments. In particular, it is trivial to perform computer experiments using functions that satisfy the criterion of a CFD theory. With all this in mind, in the present paper we only consider formulas $y = f(x)$ that can be implemented as an algorithm running on a digital computer. Using the digital computer as a metaphor guarantees that we have a well-defined precise (in terms of bits) representation of the concepts and algorithms (also in terms of bits) involved.

The purpose of the paper is to scrutinize the relation and relevance of CFD to models of EPRB experiments. We demonstrate that there exist both CFD and non-CFD-compliant computer models for the EPRB experiments that produce results in complete agreement with those of quantum theory. Because these computer models do not contain quantum concepts, CFD does not distinguish classical from quantum physics for the case of EPRB experiments.

2. Computational model

In this section we describe a loophole-free implementation of Bohm's version [7] of the EPR thought experiments [8]. This implementation simulates laboratory (EPRB) experiments with photons [2,9] but does not suffer from the practical limitations of real experiments: the computer experiments that we report upon are ideal, perfect, loophole free experiments. The computational model of the EPRB experiment is constructed such that it can reproduce, *exactly*, the single particle averages and two-particle correlations of the singlet state [10,11].

We begin by specifying the model of the observation stations which are considered to be identical computational units which operate according to a specific algorithm, see Fig. 1. Input to a unit is the setting a (representing the angle of the polarizer), an angle $0 \leq \phi < 2\pi$ (representing the polarization of the photon), and a number $0 \leq r < 1$. Output of a given unit is a binary variable $x = \pm 1$ (representing the detection event at one of the two detectors placed behind the polarizer), and a time-related parameter $0 \leq t^* \leq T$ (related to the recorded time-tag). The model parameter T is fixed and does not depend on the setting a.

Upon receiving the input (a, ϕ, r) the unit executes the following two steps [10]:

$$1.\ \text{compute}\quad c = \cos[2(a-\phi)],\ s = \sin[2(a-\phi)], \tag{1}$$

$$2.\ \text{set}\quad x = \text{sign}(c),\ t^* = rTs^2. \tag{2}$$

These two lines form the core of the computer algorithm. The simplicity of this algorithm is enticing, however, it contains several key features. One is the creation of a time-related variable t^* that has the interesting property of being a function of both the local setting a and the angle ϕ. In contrast to Bell and Clauser–Horn–Shimony–Holt (CHSH), we are dealing therefore, with time related parameters that depend on the local setting of each station. In addition, the model introduces randomness by a number $0 \leq r < 1$, distributed uniformly.

It is important to notice that the variable t^* in Eq. (2) may be imagined as being related to a "pointer-position" of a clock that symbolizes dynamic many-body interactions of the photon with the constituent particles of the source and local measurement equipment (polarizers, etc.). All of these particles perform a (relativistic) many-body "dance" that certainly may depend on the local equipment orientation as well as on properties of the incoming photons. Because this many body "dance" has never been explored in actual EPRB equipments, we consider t^* in the following only as a computer generated time-related tag that is used in order to deal selectively with the results for x after the whole computer experiment is done.

For every input event (a, ϕ, r), we know the values of all outputs variables $x = x(a, \phi)$ and $t^* = t^*(a, \phi, r)$. Therefore, the input–output relation of this unit, represented by the diagram of Fig. 1, satisfies the requirement of CFD. We also use below the somewhat simpler notation $x(a) = x(a, \phi)$ and $t^*(a) = t^*(a, \phi, r)$, keeping in mind that the x's depend on ϕ and the t^*'s depend on both ϕ and r. Here and in the following, it is implicitly understood that for every instance of new input, the values of the ϕ's and r's are generated "at random". The procedure for generating the ϕ's is specified in section "Computer simulation results".

The computational equivalent of the EPRB experiment [2,9] is shown in Fig. 2. We start by assuming that the source **S** and the observation stations $i = 1, 2$ are equipped with idealized, perfect clocks (not shown) that have been synchronized before the source is being activated. Each time the source **S** is activated, two photons are sent in opposite directions. The source is activated at times $\tau_1, \ldots, \tau_N$. We denote the minimum time interval between two emission events by $\delta\tau = \min_{n=1,\ldots,N-1}(\tau_{n+1} - \tau_n)$.

Each photon traveling to observation station $i = 1, 2$ carries its data in the form of an angle ϕ_i (representing the polarization) and a pseudo-random number $0 < r_i < 1$. The purpose of r_i is to account, be it in a highly over-simplified manner, for the influence of the many-body interactions of the incoming photon with the constituent particles of the measurement equipment (polarized beam splitter, retarders, etc.) located at observation station i, resulting in a change of the time-of-flight from the source to the detector at observation station i [5,12].

Upon arrival of photon n at station i, the observation station produces the value $x_i = \pm 1$ (see Eqs. (1) and (2)) and a time-tag

$$T_{i,n} = \tau_n + T_{\text{TOF}}^{(i)} + t_{i,n}^*, \quad i = 1, 2. \tag{3}$$

In laboratory EPRB experiments, one considers differences of time-tags only [2,13]. As the distances between the sources and the observation stations $i = 1, 2$ are fixed, we may assume that the time $T_{\text{TOF}}^{(i)}$ it takes the photon to reach the observation station i is constant. In general $T_{\text{TOF}}^{(1)} \neq T_{\text{TOF}}^{(2)}$ but the difference between the two times-of-flight may be compensated for by adding this difference

to the appropriate measured clock time $T_{i,n}$. Hence, for simplicity we assume that $T_{\rm TOF} = T^{(1)}_{\rm TOF} = T^{(2)}_{\rm TOF}$.

From Eqs. (2) and (3) it follows that $\tau_n + T_{\rm TOF} \leq T_{i,n} \leq \tau_n + T_{\rm TOF} + T$. In the following, we only consider the case $T < \delta\tau$, meaning that the maximum delay time T is smaller than the minimum time interval $\delta\tau$ between two emissions of a pair of photons. The restriction $T < \delta\tau$ implies that $\tau_n + T_{\rm TOF} \leq T_{i,n} < \tau_n + T_{\rm TOF} + \delta\tau$ and this inequality has an important consequence because it guarantees that there is a one to one correspondence between the value of the time-tag $T_{i,n}$ and the number n of the emission event. Thus, in contrast to actual experimental data [2], for the data generated by the computer model there is a one to one correspondence between the value of the time-tag $T_{i,n}$ and the number n of the emission event if the condition $T < \delta\tau$ is satisfied. With this condition we have $T_{1,n} - T_{2,n} = t^*_{1,n} - t^*_{2,n}$ and therefore, in the computer model, the time-of-flight and photon emission times $\tau_1, \ldots, \tau_N$ are superfluous and may be omitted. There is no coincidence loophole and as every photon arriving at an observation station also produces an output event $(x(a), t^*(a))$, there is no detection loophole either. Note also that the assumption $T < \delta\tau$ prevents the incorrect inclusion of impossible events, such as two different polarizer-settings for the same measurement (for details on this see [5]).

Upon arrival of the photon, observation station $i = 1, 2$ executes the algorithm defined by Eqs. (1) and (2) and produces output in the form of the pair $(x_i = \pm 1, 0 \leq t^*_i \leq T)$. The algorithm represented by Fig. 2 computes the vector-valued function

$$\begin{pmatrix} x_1 \\ t^*_1 \\ x_2 \\ t^*_2 \end{pmatrix} = \begin{pmatrix} x_1(\phi_1, a_1) \\ t^*_1(\phi_1, a_1, r_1) \\ x_2(\phi_2, a_2) \\ t^*_2(\phi_2, a_2, r_2) \end{pmatrix} = F(\phi_1, \phi_2, r_1, r_2, a_1, a_2), \tag{4}$$

hence, according to the definition of CFD, Eq. (4) defines a CFD-compliant theoretical model.

The primary aim of EPRB experiments is to demonstrate a violation of the Bell–CHSH inequality under Einstein-local conditions [14]. By construction, the computer models that we use are metaphors for Einstein-local experiments: changing a_1 (a_2) never has an effect on the values of x_2 (x_1) or t^*_2 (t^*_1), neither in the past nor in the future, hence the output of one particular unit depends on the input to that particular unit only.

The crucial point that leads to a violation of Bell's theorem is now the following. We deal with photon pairs for which an "entanglement" is defined in the Hilbert space of quantum mechanics. The correlations of the event of measurement of these pairs are, on the other hand, obtained by measurements in ordinary space and time. In other words, some criterion is employed to relate the measured pairs and identify them as belonging together. Such identification can be achieved, among other possibilities, by use of two synchronized clocks indicating time t in both measurement stations. As soon as such identification and corresponding selection of pair-measurements are implemented, we may derive a joint frequency distribution $P(T_1, T_2)$ for the time tags $T_{1,n}$ and $T_{2,n}$ for finding both $T_{1,n}$ and T_{2_n} within a time-range W around a time $t_n = \tau_n + T_{\rm TOF}$ of the synchronized station clocks. This joint frequency distribution is derived in an Einstein local way and depends on the settings of the polarizers of **both** stations, a fact that cannot be accommodated in Bell-type proofs.

Bell–CHSH inequality tests require four different experiments with different choices of the settings of the observation stations. Specifically, the setting of observation station $i = 1, 2$ can take two values which we denote by (a_i, a'_i). The choice of setting a_i or a'_i may be made at random [2,9,13]. In real experiments, it takes a certain time to switch from one setting to another but this time is less than the average time between two emission events [2]. In the computer experiment, being an idealized perfect experiment, the algorithm is such that this cannot be an issue.

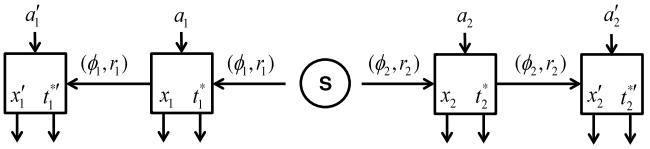

Fig. 3. Computational model for the EPRB experiment satisfying the criterion of a CFD theory.

The algorithm represented by Fig. 2 is CFD-compliant. However, the computational model represented by the diagram in Fig. 2 **cannot** compute, e.g. (x_1, x_2, x'_1, x'_2) with $x_i = x_i(a_i, \phi_i)$ and $x'_i = x'_i(a'_i, \phi_i)$ in a CFD-compliant manner: it suffers from the so-called contextuality loophole [15–17] because there is no guarantee that the random ϕ_i's used to compute the x_i's will be the same as the random ϕ_i's used for the calculation of the x'_i's. Under these circumstances the correlations calculated from the data generated by the model shown in Fig. 2 do not need to satisfy a Bell-type inequality [5,12,15,18] and, as demonstrated explicitly below through simulation, indeed they do not. Thus, the model of Fig. 2 **cannot** be used to perform a CFD-compliant simulation of the EPRB experiment.

The layout of a CFD-compliant computer model of the EPRB experiment is depicted in Fig. 3. It uses the same units as the non-CFD-compliant model shown in Fig. 2, the only difference being that the input (ϕ_i, r_i) is now fed into an observation station with setting a_i and another one with setting a'_i. As each of the four units operates according to the rules given by Eq. (1) and (2), we have $(x_1, x'_1, x_2, x'_2) = X(\phi_1, \phi_2, a_1, a'_1, a_2, a'_2)$ and $(t^*_1, t^{*\prime}_1, t^*_2, t^{*\prime}_2) = T(\phi_1, \phi_2, r_1, r_2, a_1, a'_1, a_2, a'_2)$. As the arguments of the functions X and T are independent and may take any value out of their respective domain, the whole system represented by Fig. 3 satisfies, by construction, the criterion of a CFD theory.

3. Bell–CHSH inequality and time-coincidence criterion

As CFD is used as at least one of the assumptions to prove the Bell–CHSH inequality [5], it is instructive to see how this feature appears in the computational model. Therefore, let us start by explicitly ignoring the t-variables. As is clear from Fig. 3, the two stations on the left of the source **S** receive the same data (ϕ_1, r_1) from the source. The settings a_1 and a'_1 are fixed for the duration of the N repetitions of the experiment. The same holds for the two stations at the right of the source, with subscript 1 replaced by 2. Clearly, each quadruple of output data (x_1, x'_1, x_2, x'_2) is generated in a CFD-compliant manner.

For each input event (labeled by $n = 1, \ldots, N$) we compute

$$\begin{aligned} s_n &= x_1x_2 - x_1x'_2 + x'_1x_2 + x'_1x'_2 \\ &= x_1\left(x_2 - x'_2\right) + x'_1\left(x_2 + x'_2\right), \end{aligned} \tag{5}$$

and

$$S = \frac{1}{N}\sum_{n=1}^{N} s_n \tag{6}$$

where N denotes the number of pairs that was processed by the units. From Eq. (5) it follows immediately that $|s_n| \leq 2$ and hence $|S| \leq 2$. Of course, this is what we expect: if the whole system is CFD-compliant and we ignore the t-variables, we generate quadruples and then it is impossible to violate the Bell–CHSH inequality $|S| \leq 2$ [18,19].

Next, we examine what happens if the time-tag variables $T_{i,n}$ are included. In real EPRB experiments with photons, it is essential to use time-coincidence to identify pairs [2,9,13]. The standard

procedure adopted in these experiments is to introduce a time window W and reject pairs that do not satisfy the condition $|T_{1,n} - T_{2,n}| \leq W$ (and similar for other relevant combinations of T's) [2]. The computational model defined by Eqs. (1) and (2) together with the time-coincidence criterion yields, in the limit that the time-window W vanishes, the correlation of the singlet state [10,11] if we repeat the experiment pair-wise, i.e. with four pairs of settings (see Fig. 2), in which case the CFD criterion is clearly not satisfied. We emphasize that unlike in the laboratory experiment, in the computer experiment all pairs are created "on demand", each pair is detected, and the time window only serves as a vehicle to post select pairs, not to identify them. Post-selection only serves to "probe" the complicated, time-dependent many-body physics that is involved when the photon passes through the optical system and triggers the detector. In this sense, the computer experiment suffers from none of the loopholes that may occur in experiments.

Although not feasible with photons, using the computer as a metaphor we can perform the ideal, loophole-free experiment satisfying all the requirements of a CFD theory. In the remainder of this section we discuss the ramifications to the Bell-type inequality that ensue when time is included in the description. In the next section, we demonstrate that the CFD-compliant model reproduces the quantum theoretical results of the singlet state.

We formalize the effect of the time-coincidence window by introducing the binary variables

$$\begin{aligned} w(a_1, a_2) &= \Theta(W - |T_{1,n} - T_{2,n}|) \\ w(a_1, a_2') &= \Theta(W - |T_{1,n} - T_{2,n}'|) \\ w(a_1', a_2) &= \Theta(W - |T_{1,n}' - T_{2,n}|) \\ w(a_1', a_2') &= \Theta(W - |T_{1,n}' - T_{2,n}'|), \end{aligned} \tag{7}$$

where $\Theta(x)$ is the unit step function. In essence, we extend the computational device by taking the output of the two units described earlier and feeding the time-tag output in a "correlator" that computes, for each event n, the four binary variables defined by Eq. (7). Adding the correlator does not change the fact that the computer model is CFD-compliant. Indeed, a given input $(\phi_1, r_1, \phi_2, r_2)$ together with the settings (a_1, a_1', a_2, a_2') completely determines the values of all (two-valued) output variables $x(a_1), x(a_1'), x(a_2), x(a_2'), w(a_1, a_2), w(a_1, a_2'), w(a_1', a_2)$, and $w(a_1', a_2')$. Note that e.g. $w(a_1, a_2) = 0$ means that the particular pair has been discarded by the time-coincidence criterion for the pair of settings (a_1, a_2) but that this does not imply that e.g. $w(a_1, a_2') = 0$. In other words, the values of the w's are used to post-select pairs.

Next we compute averages and correlations of the coincident pairs as is done in laboratory EPRB experiments [2]. The single-x averages and correlation for the settings (a_1, a_2) are defined by

$$\begin{aligned} E_1(a_1, a_2) &= \frac{\sum w(a_1, a_2) x(a_1)}{\sum w(a_1, a_2)} \\ E_2(a_1, a_2) &= \frac{\sum w(a_1, a_2) x(a_2)}{\sum w(a_1, a_2)} \\ E(a_1, a_2) &= \frac{\sum w(a_1, a_2) x(a_1) x(a_2)}{\sum w(a_1, a_2)}, \end{aligned} \tag{8}$$

and we have similar expressions for the other choices of settings. In Eq. (8) it is understood that $\sum$ means $\sum_{n=1}^{N}$, i.e. the sum over all input events, characterized by values of the r's and ϕ's. It is not difficult to see that $E_1(a_1, a_2)$, $E_2(a_1, a_2)$, etc. are zero, up to fluctuations. The reason is that $\phi \to \phi + \pi/2$ changes the sign of the x's but has no effect on the values of the t^*'s (see Eq. (2)). Therefore, if the $\phi's$ uniformly cover $[0, 2\pi[$, the number of times $x = +1$ and $x = -1$ appear is about the same.

The usual strategy of deriving a Bell-like inequality for $S = E(a_1, a_2) - E(a_1, a_2') + E(a_1', a_2) + E(a_1', a_2')$ does not work simply because not all w's need to be one for the same event n [12] but we can, without using probability theory, derive another inequality by following the strategy of Larsson and Gill [20]. Denoting the number of input events for which the four pairs of settings simultaneously satisfy the coincidence criterion by N' and the maximum number of pairs per setting that satisfies the coincidence criterion by $N_{\max}$, we have $0 \leq \delta \equiv N'/N_{\max} \leq 1$ and it is straightforward to show (by repeated application of the triangle inequality) that the following statement holds: in the case that the time-coincidence criterion is used to post-select pairs, the correlations cannot violate the inequality

$$\left|E(a_1, a_2) - E(a_1, a_2') + E(a_1', a_2) + E(a_1', a_2')\right| \leq 4 - 2\delta. \tag{9}$$

Therefore, if the algorithm generates all the variables strictly in accordance with the criterion of a CFD theory, using the time-coincidence window to post-select pairs does not lead to the Bell–CHSH inequality unless $\delta = 1$ in which case all w's are equal to one and none of the pairs are discarded by the post-selection procedure. The term 2δ in Eq. (9) is a measure for the number of pairs that have been post-selected relative to the number of emitted pairs.

At this point, it is important to mention that in establishing Eq. (9), the specific computational model that we have used as a concrete realization is not essential: as long as the algorithm generates x's and T's in accordance with the criterion of a CFD theory and $\delta > 0$, Eq. (9) holds.

4. Computer simulation results

As explained earlier, from the logical structure of the algorithm it is evident that the outcome of a particular unit cannot be influenced by the input/output of another unit, neither by the current input event nor by past or future events. Therefore, all models that we consider generate data by a process that complies with the notion of Einstein locality.

We present the results of four different modes of simulating the EPRB experiments. This section reports the results of simulations for 100 repetitions of the EPRB experiment with $N = 10^6$ events per pair of settings in the case of the non-CFD-compliant models and $N = 4 \times 10^6$ events for the CFD-compliant models. We set $\phi_1 = \phi$ and $\phi_2 = \phi + \pi/2$ where $0 \leq \phi < 2\pi$ is a uniform pseudo-random number, corresponding to the case in which the polarizations of the two photons within a pair are orthogonal and fully correlated (if ϕ_1 and ϕ_2 are uncorrelated and random, the average of the x's and the average of e.g. $x_1 x_2$ are all zero, independent of the settings). The algorithm of the unit simulating the observation station is defined by Eqs. (1) and (2). For the settings we take $a_1 = 0, a_1' = \pi/4, a_2 = \pi/8, a_2' = 3\pi/8$ as these are known to be a choice that maximizes S, for the time window we take $W = 1$ and the maximum time delay is taken to be $T = 1000$.

Case 1: non-CFD-compliant model (see Fig. 2), no post selection by a time window. The averages and correlations are obtained from four sets of measurements with the four different pairs of settings (a_1, a_2), (a_1, a_2'), (a_1', a_2), and (a_1', a_2'). As the output of the stations with say setting (a_1, a_2) is not available when the experiment runs with another setting, say (a_1, a_2'), this computer experiment does not satisfy the criterion of a CFD theory, nor does it mimic a real EPRB experiment with photons. For a set of 100 repetitions, the simulations show that 54 out of 100 repetitions yield a violation of $|S| \leq 2$. The average of S being 2.0000 with standard deviation 0.0016. Therefore, in a mathematically strict sense, for finite N, the non-CFD-compliant model without post selection by

a time window yields data that violates the inequality $|S| \leq 2$, as expected [12]. However, this model does not yield the correlation that is characteristic for a quantum system in the singlet state.

Case 2: **non-CFD-compliant model** (**see** Fig. 2), **post selection by a time window.** The averages and correlations are obtained from four sets of measurements with four different pairs of settings (a_1, a_2), (a_1, a_2'), (a_1', a_2), and (a_1', a_2'). This computer experiment does not satisfy the criterion of a CFD theory. Models that incorporate post selection are known to produce results that violate $|S| \leq 2$ [10,21–27]. For a set of 100 repetitions, the simulations show that 100 out of 100 repetitions yield a violation of $|S| \leq 2$, the average of S being 2.824 with standard deviation 0.032. This value of S is very close to the theoretical maximum $2\sqrt{2} = 2.8284$ for the quantum system in the singlet state [28].

Case 3: **CFD-compliant model** (**see** Fig. 3), **no post selection by a time window.** If the averages and correlations are obtained from sets of quadruples (x_1, x_1', x_2, x_2'), the model is CFD-compliant and the CHSH inequality $|S| \leq 2$ cannot be violated. For the same set of 100 repetitions as used in Case 1, the simulations always yield $|S| = 2$, hence the CHSH inequality is satisfied, as it should be.

Case 4: **CFD-compliant model** (**see** Fig. 3), **post selection by a time window.** If the averages and correlations are obtained from sets of quadruples (x_1, x_1', x_2, x_2') post-selected by way of the time-coincidence criterion, the CHSH inequality cannot be derived and the correlations satisfy instead Eq. (9). For the same set of 100 repetitions as used in Case 1, the simulations show that 100 out of 100 repetitions yield a violation of $|S| \leq 2$, the average of S being 2.827 with standard deviation 0.016. This value of S is very close to the theoretical maximum $2\sqrt{2} = 2.8284$ for the quantum system in the singlet state [28]. The minimum value of δ found in these 100 repetitions is 0.14×10^{-3}, that is the number of pairs rejected by the time-coincidence criterion is significant. Note that unlike case 2, it is impossible to perform this CFD-compliant experiment with photons.

In Fig. 4 we show the correlation $E(a_1, a_2)$ and single-x averages as obtained from the simulation with the CFD-compliant model with post selection. Quantum theory predicts $E(a_1, a_2) = -\cos[2(a_1 - a_2)]$. From Fig. 4 it is clear that the CFD-compliant model reproduces the results of quantum theory without making any reference to the latter.

5. Conclusion

A CFD-compliant model of the EPRB experiment that incorporates post-selection by a time window can violate the inequality $|S| \leq 2$ but cannot violate Eq. (9). Furthermore, with the proper choice of model parameters, this model reproduces the results of the quantum theoretical description of the EPRB experiment in terms of the singlet state. Therefore, we have demonstrated that in the case of the EPRB experiment, CFD does not separate or distinguish classical from quantum physics. The CFD-compliant model, which may be viewed as having physical time involved in the post-selection process as a hidden variable, provides a counterexample to the dogma that CFD implies a Bell-type inequality.

In summary, we have presented a simulation model that provides a counterexample, to the incorrect (but generally held) belief that any Einstein-local and counterfactually-definite model cannot produce results that are commonly considered to be a signature of genuine quantum behavior.

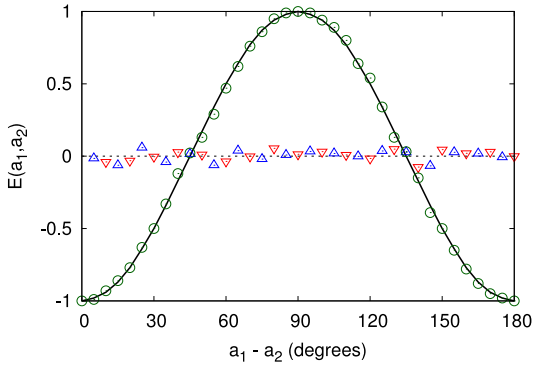

Fig. 4. The correlation $E(a_1, a_2)$ (◯) and single-x averages $E_1(a_1, a_2)$ (△) and $E_2(a_1, a_2)$ (▽) as a function of $a_1 - a_2$ as obtained from computer simulation data of the CFD-compliant model (see Fig. 3) with time-coincidence window $W = 1$ and $T = 1000$. Solid line: quantum theoretical result of the correlation $E(a_1, a_2)$ of a quantum system in the singlet state. Dashed line: quantum theoretical result of the single-x averages $E_1(a_1, a_2) = E_2(a_1, a_2) = 0$ in the singlet state.

Appendix. Derivation of Eq. (9)

First we decompose the sum over all n into a sum over all n's for which $w(a_1, a_2)w(a_1, a_2')w(a_1', a_2)w(a_1', a_2') = 1$ (i.e. all input events for which the four pairs of settings yield coincidences) and denote this sum by $\sum'$. The sum over all n's for which $w(a_1, a_2)w(a_1, a_2')w(a_1', a_2)w(a_1', a_2') = 0$ is denoted by $\sum''$. Thus, we have $\sum = \sum' + \sum''$.

By the definition of $\sum'$ we have $N' = \sum' w(a_1, a_2) = \sum' w(a_1', a_2) = \sum' w(a_1, a_2') = \sum' w(a_1', a_2') = \sum' 1 \leq N$. Clearly, N' is nothing but the number of quadruples generated by the algorithm. The maximum of the number of pairs per setting that satisfies the time-coincidence criterion is given by $N_{\max} = \max\left[\sum w(a_1, a_2), \sum w(a_1', a_2), \sum w(a_1, a_2'), \sum w(a_1', a_2')\right] > 0$, whereby we exclude the case that the time-coincidence criterion rejects all events for all settings. Considering the four different settings, the minimum of the ratio of quadruples over pairs that satisfies the time-coincidence criterion is $\delta = N'/N_{\max}$. Obviously, we have $0 \leq \delta \leq 1$.

Using the definition of $\sum'$ and $\sum''$ we can write, for instance,

$$\begin{aligned} E(a_1, a_2) &= \frac{\sum w(a_1, a_2)x(a_1)x(a_2)}{\sum w(a_1, a_2)} \\ &= \frac{\sum' w(a_1, a_2)x(a_1)x(a_2) + \sum'' w(a_1, a_2)x(a_1)x(a_2)}{\sum w(a_1, a_2)} \\ &= \frac{\sum' w(a_1, a_2)x(a_1)x(a_2)}{\sum' w(a_1, a_2)} \frac{\sum' w(a_1, a_2)}{\sum w(a_1, a_2)} \\ &\quad + \frac{\sum'' w(a_1, a_2)x(a_1)x(a_2)}{\sum'' w(a_1, a_2)} \frac{\sum'' w(a_1, a_2)}{\sum w(a_1, a_2)} \\ &= E'(a_1, a_2)\frac{\sum' w(a_1, a_2)}{\sum w(a_1, a_2)} + E''(a_1, a_2)\frac{\sum'' w(a_1, a_2)}{\sum w(a_1, a_2)}, \end{aligned} \tag{10}$$

where

$$\begin{aligned} E'(a_1, a_2) &= \frac{\sum' w(a_1, a_2)x(a_1)x(a_2)}{\sum' w(a_1, a_2)}, \\ E''(a_1, a_2) &= \frac{\sum'' w(a_1, a_2)x(a_1)x(a_2)}{\sum'' w(a_1, a_2)}. \end{aligned} \tag{11}$$

Next, we rewrite Eq. (10) as

$$\begin{aligned} E(a_1, a_2) - \delta E'(a_1, a_2) &= E'(a_1, a_2)\left[\frac{\sum' w(a_1, a_2)}{\sum w(a_1, a_2)} - \delta\right] \\ &\quad + E''(a_1, a_2)\frac{\sum'' w(a_1, a_2)}{\sum w(a_1, a_2)}, \end{aligned} \tag{12}$$

and as (by definition)

$$\frac{\sum' w(a_1,a_2)}{\sum w(a_1,a_2)} \geq \frac{\sum' w(a_1,a_2)}{N_{\max}} = \frac{N'}{N_{\max}} = \delta, \tag{13}$$

using the triangle inequality and the trivial bounds $\left|E'(a_1,a_2)\right| \leq 1$ and $\left|E''(a_1,a_2)\right| \leq 1$ yields

$$\begin{aligned}
\left|E(a_1,a_2) - \delta E'(a_1,a_2)\right| &\leq \left|E'(a_1,a_2)\right| \left[\frac{\sum' w(a_1,a_2)}{\sum w(a_1,a_2)} - \delta\right] \\
&\quad + \left|E''(a_1,a_2)\right| \frac{\sum'' w(a_1,a_2)}{\sum w(a_1,a_2)} \\
&\leq \frac{\sum' w(a_1,a_2)}{\sum w(a_1,a_2)} - \delta + \frac{\sum'' w(a_1,a_2)}{\sum w(a_1,a_2)} \\
&\leq \frac{\sum' w(a_1,a_2) + \sum'' w(a_1,a_2)}{\sum w(a_1,a_2)} - \delta \\
&\leq 1 - \delta. \qquad (14)
\end{aligned}$$

It is easy to see that for the other settings we have the same upperbound as in Eq. (14). Using the triangle inequality once more we have

$$\begin{aligned}
&\left|E(a_1,a_2) - E(a_1,a_2') + E(a_1',a_2) + E(a_1',a_2')\right| \\
&= \left|E(a_1,a_2) - \delta E'(a_1,a_2) - E(a_1,a_2') + \delta E'(a_1,a_2')\right. \\
&\quad + E(a_1',a_2) - \delta E'(a_1',a_2) + E(a_1',a_2') - \delta E'(a_1',a_2') \\
&\quad \left. + \delta[E'(a_1,a_2) - E'(a_1,a_2') + E'(a_1',a_2) + E'(a_1',a_2')]\right| \\
&\leq \left|E(a_1,a_2) - \delta E'(a_1,a_2)\right| + \left|E(a_1,a_2') - \delta E'(a_1,a_2')\right| \\
&\quad + \left|E(a_1',a_2) - \delta E'(a_1',a_2)\right| + \left|E(a_1',a_2') - \delta E'(a_1',a_2')\right| \\
&\quad + \delta\left|E'(a_1,a_2) - E'(a_1,a_2') + E'(a_1',a_2) + E'(a_1',a_2')\right| \\
&\leq 4(1-\delta) + 2\delta = 4 - 2\delta, \qquad (15)
\end{aligned}$$

where we used the fact that $\left|E'(a_1,a_2) - E'(a_1,a_2') + E'(a_1',a_2) + E'(a_1',a_2')\right| \leq 2$ because these correlations only involve pairs that satisfy the time-coincidence criterion. Note that we recover the CHSH inequality only if $\delta = 1$, that is only if $w(a_1,a_2)w(a_1,a_2')w(a_1',a_2)w(a_1',a_2') = 1$ for all n or, in other words, only if the time-coincidence criterion does not reject pairs. For $\delta = 0$ we recover the trivial inequality $\left|E(a_1,a_2) - E(a_1,a_2') + E(a_1',a_2) + E(a_1',a_2')\right| \leq 4$.

References

[1] D.P. Landau, K. Binder, A Guide to Monte Carlo Simulation in Statistical Physics, Cambridge University Press, Cambridge, 2000.
[2] G. Weihs, T. Jennewein, C. Simon, H. Weinfurther, A. Zeilinger, Phys. Rev. Lett. 81 (1998) 5039–5043.
[3] E.E. Rosinger, Do quanta violate the equation 0 = 0? arXiv:1604.0211v3.
[4] J. Pearl, Causality: Models, Reasoning, and Inference, Cambridge University Press, Cambridge, 2000.
[5] K. Hess, H. De Raedt, K. Michielsen, J. Mod. Phys. (2016) in press, arXiv:1605.04889.
[6] A. Peres, Quantum Theory: Concepts and Methods, Kluwer Academic Publishers, Dordrecht, Boston, London, 1995.
[7] D. Bohm, Quantum Theory, Prentice-Hall, New York, 1951.
[8] A. Einstein, A. Podolsky, N. Rosen, Phys. Rev. 47 (1935) 777–780.
[9] A. Aspect, J. Dalibard, G. Roger, Phys. Rev. Lett. 49 (1982) 1804–1807.
[10] K. De Raedt, K. Keimpema, H. De Raedt, K. Michielsen, S. Miyashita, Eur. Phys. J. B 53 (2006) 139–142.
[11] K. Michielsen, H. De Raedt, Internat. J. Modern Phys. C 25 (2014) 01430003.
[12] K. Hess, H. De Raedt, K. Michielsen, Adv. Math. Phys. (2016) in press, arXiv:1605.04887.
[13] B. Hensen, H. Bernien, A.E. Dreau, A. Reiserer, N. Kalb, M.S. Blok, J. Ruitenberg, R.F.L. Vermeulen, R.N. Schouten, C. Abellan, W. Amaya, V. Pruneri, M.W. Mitchell, M. Markham, D.J. Twitchen, D. Elkouss, S. Wehner, T.H. Taminiau, R. Hanson, Nature (2015) 15759.
[14] J.S. Bell, On the Foundations of Quantum Mechanics, World Scientific, Singapore, New Jersey, London, Hong Kong, 2001.
[15] T.M. Nieuwenhuizen, Found. Phys. 41 (2011) 580–591.
[16] M. Kupczyński, Phys. Lett. A 121 (1987) 205–207.
[17] M. Kupczyński, J. Russ. Laser Res. 26 (2005) 514–523.
[18] H. De Raedt, K. Hess, K. Michielsen, J. Comput. Theor. Nanosci. 8 (2011) 1011–1039.
[19] G. Boole, Phil. Trans. R. Soc. Lond. 152 (1862) 225–252.
[20] J.-Å. Larsson, R.D. Gill, Europhys. Lett. 67 (2004) 707–713.
[21] P.M. Pearle, Phys. Rev. D 2 (1970) 1418–1425.
[22] A. Fine, Synthese 29 (1974) 257–289.
[23] S. Pascazio, Phys. Lett. A 118 (1986) 47–53.
[24] C. Brans, Internat. J. Theoret. Phys. 27 (1987) 219–226.
[25] K. De Raedt, H. De Raedt, K. Michielsen, Comput. Phys. Comm. 176 (2007) 642–651.
[26] S. Zhao, H. De Raedt, K. Michielsen, Found. Phys. 38 (2008) 322–347.
[27] A. Khrennikov, Found. Phys. 45 (2015) 711–725.
[28] B.S. Cirel'son, Lett. Math. Phys. 4 (1980) 93–100.